CrystEngComm

Accepted Manuscript

Journal Name RSCPublishing

ARTICLE

Syntheses, Topological Structures and Properties of Six Metal-Organic Frameworks Constructed by the Flexible Tetracarboxylate Ligand

Cite this: DOI: 10.1039/x0xx00000x

Received 00th January 20xx
Accepted 00th January 20xx

DOI: 10.1039/x0xx00000x

www.rsc.org/

Yu Peng, Guanghua Li, Jia Hua, Zhan Shi*, and Shouhua Feng

Six new metal-organic frameworks (MOFs), $Co_2O(odip)(py)_2(DMSO)_2\cdot 3H_2O$ (**1**), $Co_2(odip)(H_2O)(DMA)_2\cdot 2DMA$ (**2**), $Co_4(odip)_2(H_2O)_4(DMSO)_2\cdot 5DMSO$ (**3**), $[Zn_2(odip)(DMF)_2(H_2O)]\cdot 2DMF\cdot 2H_2O$ (**4**), $Zn_2(odip)(H_2O)$ (**5**) and In(odip)·3ACN (**6**), have been synthesized from the 5,5'-oxydiisophthalic acid (H_4odip) ligand under solvothermal conditions. These six compounds were characterized by single-crystal X-ray diffraction, power X-ray diffraction and relative physical methods. MOFs **1**, **2** and **3** are constructed from the same ligand and metal-salt under the same temperature, but with different solvent, and they exhibit three different topologies. MOF **1** possesses a 3D 4-coordinated architecture with $(6^5\cdot 8)$ topology. MOF **2** features a 3D 4-coordinated net with $(4^2\cdot 6^3\cdot 8)$ topology and MOF **3** shows a 3D 4-coordinated framework with $(4\cdot 6^4\cdot 8)(4\cdot 6^5)$ topology. MOFs **4** and **6** have the same topology as MOF **2**. MOF **5** exhibits a 3D 5-coordinated framework with $(4^4\cdot 6^6)$ topology. These results indicate that the solvent environment plays important roles in the formation of the final framework. Moreover, the photoluminescence properties of **4** and **5**, and the magnetic properties of **1**, **2** and **3** have been studied and discussed.

Introduction

Over the past decades, metal-organic frameworks (MOFs) have attracted much interest because of their unique structural topologies[1] and wide range of potential applications in the fields of gas adsorption/separation[2], magnetism[3], catalysis[4], luminescence[5]and drug delivery[6]. Although the structure of MOFs mainly depends on the metal ions (or metal clusters) and organic ligand[7], many other factors may also affect the final structure, such as the reaction temperature, the ratio of reagents, pH value and solvents[8]. Among these factors, the solvents in particular can affect the configuration of the ligand and coordinate to the metal ions, influencing the topological structure of the final compounds. By closely controlling the solvent, metal-organic frameworks with fantastic structures and desirable properties can be synthesized[8f]. To date, much effort has been devoted to the rational design of rigid multidentate ligands[9], such as polycarboxylate ligands and N-heterocyclic ligands due to their rich coordination modes, to afford unpredictable and high-connected networks with large pores[10]. Compared with the rigid ligands, the conformation of the flexible polycarboxylate ligands can be easily affected by external factors, which makes it possible to coordinate different metal ions or metal clusters with unusual topologies and special properties[11]. Meanwhile, the flexible ligand itself can be easily twisted and rotated in the self-assembly process[12]. Although many studies have focused on the design and synthesis of flexible ligands to prepare new compounds, it is still a great challenge for chemists to fully understand the relationships between configuration and topology.

Recently, our group has been investigating MOFs constructed from polycarboxylic acid flexible ligands bridged by imino or ether group, which exhibited great adsorption behaviors and high catalytic activities[13]. In order to obtain more information on the flexible ligand, we designed and synthesized the 5, 5'-oxydiisophthalic acid (H_4odip) as a functional ligand (Scheme 1). The H_4odip molecule has flexible ether group between the benzene rings, which affords the ligand flexible conformations. Meanwhile, it also enhances the topologies of the final compounds. In this research, we

report on the synthesis and structure of six novel 3D metal-organic frameworks, $Co_2O(odip)(py)_2(DMSO)_2\cdot 3H_2O$ (**1**), $Co_2(odip)(H_2O)(DMA)_2\cdot 2DMA$ (**2**), $Co_4(odip)_2(H_2O)_4(DMSO)_2\cdot 5DMSO$ (**3**), $[Zn_2(odip)(DMF)_2(H_2O)]\cdot 2DMF\cdot 2H_2O$ (**4**), $Zn_2(odip)(H_2O)$ (**5**) and $In(odip)\cdot 3ACN$ (**6**). Furthermore, the photoluminescence properties of **4** and **5**, and the magnetic properties of **1**, **2** and **3** will also be discussed.

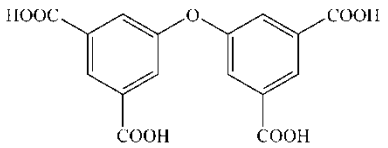

Scheme 1 Structure of the H_4odip ligand.

Experimental

Materials and methods

All the reagents employed were commercially available and used without further purification. The powder X-ray diffraction (PXRD) data were collected using a Rigaku D/max2550 diffractometer with Cu Kα radiation (λ=1.5418 Å). Elemental analyses (C, H, N and S) were done using a Perkin-Elmer 2400. The thermogravimetric analyses (TGA) were performed on TGA Q500 under air flow with a heating rate of 10 ℃ min^{-1}. Fourier transform infrared (IR) spectra were measured within the 400-4000 cm^{-1} region using a Bruker IFS-66 V/S FT-IR spectrometer. The fluorescence spectra were obtained using a FLUOROMAX-4 fluorescence spectrometer in the solid state at room temperature. The magnetic measurements of the compounds were carried out using a Quantum Design SQUID MPMS-VSM magnetometer in the temperature range of 2–300 K for fields up to 5 T.

Synthesis of 5,5'-oxydiisophthalic acid (H_4odip)

H_4odip was prepared according to the literature method.[14] 5-Hydroxy-isophthatic acid diethyl ester (3.55g, 25mmol) and K_2CO_3 (3.00g, 22mmol) were added to a 100 mL round-bottom flask, and then 25 mL DMF was added. The mixture was stirred for a while at 80 °C. Then 3,5-Dicyanofluorobenzene (2.68g, 18mmol) was added to the flask. The mixture was stirred at 80 °C for 36 h. The resulting solution was poured into 150 mL ice-cold water and white solid precipitated dimethyl 5-(3,5-dicyanophenoxy) isophthalate was collected by filtration. Dimethyl 5-(3,5-dicyanophenoxy)isophthalate (3.3g 10mmol) and 6(N) NaOH solution (60mL) were refluxed overnight. The pH value was adjusted to approximately 4 using hydrochloric acid. The resulting white precipitate was collected by filtration, washed with water, and dried under vacuum to yield 5,5'-oxydiisophthalic acid (H_4odip) (2.5 g, 70%). 1H NMR (DMSO-d6): δ 5.75 (s, 2H), 5.22 (d, 4H).

Synthesis of $Co_2O(odip)(py)_2((DMSO)_2\cdot 3H_2O$(1).

$Co(ClO_4)_2\cdot 6H_2O$ (0.0265g, 0.1 mmol) and H_4odip (0.0348 g, 0.1 mmol) were mixed in 1 mL pyridine and 1 mL DMSO. The mixture was placed in a 20 mL vial and heated at 80 °C for 1 day, and then the mixture was cooled to room temperature. Pink crystals were collected and dried in air (36% yield based on $Co(ClO_4)_2\cdot 6H_2O$). Elemental analysis (wt%) for **4**: calcd: C, 45.58, H 3.57, N 3.54, S 8.11. Found: C 45.64, H 3.82, N 3.78, S 8.24. IR (KBr, cm^{-1}): 3422, 3072, 1630, 1566, 1449, 1373, 1252, 1210, 1119, 1039, 914, 781, 701, 621, 553, 458.

Synthesis of $Co_2(odip)(H_2O)(DMA)_2\cdot 2DMA$ (2).

$Co(ClO_4)_2\cdot 6H_2O$ (0.0259g, 0.1 mmol) and H_4odip (0.0336 g, 0.1 mmol) were mixed in 1 mL water and 4 mL DMA. The mixture was placed in a 20 mL vial and heated at 80 °C for 2 day, and then the mixture was cooled to room temperature. Pink crystals were collected and dried in air (64% yield based on $Co(ClO_4)_2\cdot 6H_2O$). Elemental analysis (wt%) for **5**: calcd: C, 44.18, H 4.07, N 4.29. Found: C 44.95, H 3.95, N 4.57. IR (KBr, cm^{-1}): 3327, 3087, 2925, 1953, 1608, 1563, 1454, 1373, 1251, 1004, 913, 773, 713, 451.

Synthesis of $Co_4(odip)_2(H_2O)_4(DMSO)_2\cdot 5DMSO$ (3).

$Co(ClO_4)_2\cdot 6H_2O$ (0.0263g, 0.1 mmol) and H_4odip (0.0354 g, 0.1 mmol) were mixed in 1 mL water and 4 mL DMSO. The mixture was placed in a 20 mL vial and heated at 80 °C for 2 day, and then the mixture was cooled to room temperature. Pink crystals were collected and dried in air (73% yield based on $Co(ClO_4)_2\cdot 6H_2O$). Elemental analysis (wt%) for **6**: calcd: C, 35.89, H 2.67, N 4.65, S 5.32. Found: C 3595, H 3.95, N 4.57, S 5.45. IR (KBr, cm^{-1}): 3411, 3082, 3008, 2913, 1623, 1571, 1454, 1402, 1322, 1248, 1102, 1000, 948, 787, 720, 574, 450.

Synthesis of $[Zn_2(odip)(DMF)_2(H_2O)]\cdot 2DMF\cdot 2H_2O$ (4).

$ZnCl_2$ (0.0273g, 0.2 mmol) and H_4odip (0.0346 g, 0.1 mmol) were mixed in 4 mL DMF and 1 mL water. The mixture was placed in a 20 mL vial and heated at 80 °C for 3 days, and then the mixture was cooled to room temperature. Colorless crystals were collected and dried in air (68% yield based on $ZnCl_2$). Elemental analysis (wt%) for **2**: calcd: C, 42.93, H 4.63, N 56.03. Found: C 43.15, H 4.58, N 56.27. IR (KBr, cm^{-1}): 3272, 1674, 1564, 1465, 1377, 1259, 1107, 1009, 914, 777, 717, 454.

Synthesis of $Zn_2(odip)(H_2O)$ (5).

$Zn(NO_3)_2\cdot 6H_2O$ (0.0297g, 0.1 mmol) and H_4odip (0.0356 g, 0.1 mmol) were mixed in 4 mL DMF and 1 mL acetonitrile. The mixture was placed in a 20 mL vial and heated at 80 °C for 2 days, and then the mixture was cooled to room temperature. Colorless crystals were collected and dried in air (43% yield based on $Zn(NO_3)_2\cdot 6H_2O$). Elemental analysis (wt%) for **3**: calcd: C, 39.29, H 1.24. Found: C 39.35, H 1.42. IR (KBr, cm^{-1}): 3383, 3076, 2929, 1668, 1566, 1452, 1380, 1259, 1107, 1012, 989, 925, 788, 723, 454.

Table 1 Crystal Data and Structure Refinements for Complexes 1−6

Compounds	**1**	**2**	**3**	**4**	**5**	**6**
Empirical formula	$C_{30}H_{34}Co_2N_2O_{15}S_2$	$C_{32}H_{44}Co_2N_4O_{14}$	$C_{46}H_{62}Co_4N_4O_{29}S_7$	$C_{28}H_{40}Zn_2N_4O_{16}$	$C_{16}H_6Zn_2O_{10}$	$C_{22}H_{15}InN_3O_9$
Formula weight	844.57	826.57	1539.10	819.38	488.95	580.19
Crystal	Triclinic	Orthorhombic	Monoclinic	Monoclinic	Monoclinic	Orthorhombic
Space group	$P3_121$	$P2_12_12_1$	$P2_1/c$	$P2_1/c$	$C2/c$	$Pnma$
a/Å	19.851(3)	10.1170(11)	21.818(4)	10.289(2)	19.005(4)	17.303(4)
b/Å	19.851(3)	16.767(2)	14.704(3)	15.763(3)	13.683(3)	9.925(2)
c/Å	9.876(2)	22.415(2)	26.282(5)	24.796(5)	14.521(3)	22.410(5)
α/(°)	90	90	90	90	90	90
β/(°)	90	90	126.84(3)	112.65(3)	119.11(3)	90
γ/(°)	120	90	90	90	90	90
Volume/Å^3	3370.6(10)	3802.3(7)	6748(2)	3711.4(13)	3299.2(11)	3848.3(13)
Z	3	4	4	4	8	4
D_{calc}, g/cm^3	1.248	1.402	1.515	1.466	1.969	1.001
μ/ m m^{-1}	0.888	0.939	1.261	1.365	2.966	0.649
F(000)	1302	1672	3160	1696	1936	1156
GOF	1.073	1.012	1.041	1.083	1.068	1.132
Flack	0.08(5)	0.03(3)				
R_1 ^{a}wR$_2$ ^{b}[I>2σ(I)]	R1=0.0951, wR2=0.2540	R1=0.0778, wR2=0.1563	R1=0.1127, wR2=0.2865	R1=0.0674, wR2=0.1987	R1=0.0301, wR2=0.0784	R_1=0.0700, wR$_2$=0.2562
R_1 ^{a} wR$_2$ ^{b}(All data)	R1=0.1136, wR2=0.2646	R1=0.1758, wR2=0.1796	R1=0.1223, wR2=0.2943	R1=0.0918, wR2=0.2133	R1=0.0357, wR2=0.0809	R1 =0.0848, wR2 =0.2692

$^aR_1 = ||F_o| - |F_c||/\Sigma|F|_o$. ^{b} $wR_2 = [\Sigma w(F_o^2 - F_c^2)^2/\Sigma w(F_o^2)^2]^{1/2}$.

Synthesis of In(odip)·3ACN **(6)**.
$In(NO_3)_3 \cdot 4H_2O$ (0.0391g, 0.1 mmol) and H_4odip (0.0346g, 0.1 mmol) were mixed in 4 mL DMF and 1 mL acetonitrile. The mixture was placed in a 20 mL vial and heated at 80 °C for 12 hours, and then the mixture was cooled to room temperature. Colorless crystals were collected and dried in air (57% yield based on $In(NO_3)_3 \cdot 4H_2O$). Elemental analysis (wt%) for **1**: calcd: C, 41.86, H 1.76. Found: C 41.79, H 1.96. IR (KBr, cm^{-1}): 3089, 2802, 1658, 1575, 1471, 1390, 1255, 1122, 995, 777, 701.

The phase purity of samples was confirmed by the experimental PXRD and the calculated patterns (see the ESI Fig. S1-S6). For the six MOFs, all the peaks are in accordance with the simulated PXRD patterns, indicating that all of the MOFs have a pure phase.

X-ray crystallography

Single-crystal X-ray data for MOFs **1**and **4-6** were collected using a Rigaku RAXIS-RAPID equipped with a 5.4 kW sealed tube X- ray source (graphite-monochromated Mo-Kα radiation, λ= 0.71073Å). The data processing was accomplished with the PROCESS-AUTO processing program. MOFs **2** and **3** were performed on a Bruker Smart-1000 CCD area detector-equipped diffractometer with graphite-monochromated Mo-Kα (λ= 0.71073Å). Empirical absorption correction was applied. All of the data were collected at a temperature of 20 ±2 °C. The structures were solved by direct methods and refined by the full-matrix least-squares methods on F^2 using the SHELXTL-97 crystallographic software package[15]. All non-hydrogen atoms were found from difference Fourier map and refined anisotropically. All of the hydrogen atoms from the ligand were placed in the calculated positions, and hydrogen atoms of the water molecules or solvent molecules that were not be included in the model were included in the structure factor calculation. The solvent

molecules in MOFs **1-4**, and **6** were highly disordered and were removed from the diffraction data by using the SQUEEZE routine of PLATON[16]. The final formulas were derived from the crystallographic data combined with elemental and thermogravimetric analysis data. The basic crystallographic data information of MOFs **1-6** is summarized in Table 1. Topology information for the three compounds was calculated with TOPOS 4.0[17].

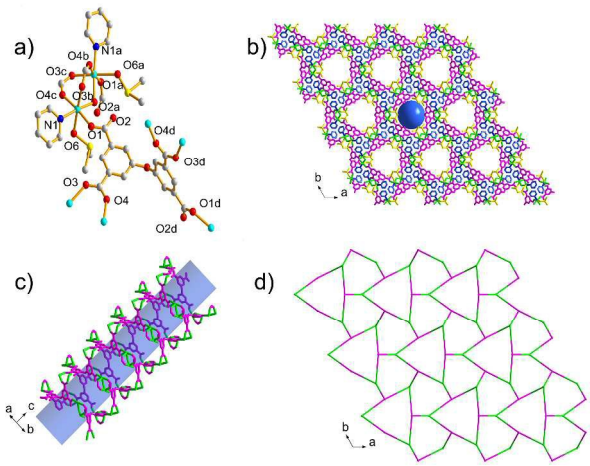

Figure 1 (a) The coordination environment of Co and the bonding mode of the H_4odip in MOF **1**. All H atoms are omitted for clarity. The atoms with superscript 'a' are related by (1+x-y,2-y,0.66667-z), 'b' are related by (1-y,1+x-y,0.33333+z), 'c' are related by (1-x,1-x+y,0.33333-z) and 'd' are related by (y,x,1-z); (b) The 3D framework of MOF **1**; (c) 1D channel along the *c* axis; (d) Schematic representation of topological net of MOF **1**.

$Co_2O(odip)(py)_2((DMSO)_2 \cdot 3H_2O$ (1). MOF **1** displays in trigonal crystal system and space group *P3₁21* with a 4-coordinated 3D framework. The asymmetric unit of MOF **1** contains half crystallographically independent Co^{2+} atom, half bridging oxygen atom, half $odip^{4-}$ ligand, one py molecule and two half-occupancy DMSO molecules which share a common unit-occupancy oxygen atom. In fact, in the refinement of the structure, the temperature factor rate of the half-occupancy DMSO is relatively high. We try to refine the DMSO as four quarter-occupancy DMSO molecules, but the result is not ideal. Here further refinement was not made, the configuration of DMSO molecule does not affect the coordination mode of Co1. As shown in Figure 1a, Co1 is coordinated to one nitrogen atom from py molecule, and three oxygen atoms belonging to three different carboxyl oxygen atoms of three $odip^{4-}$ ligands, one oxygen atom from DMSO molecule and one bridging oxygen atom. The coordination geometry of the Co1 can be described as octahedron, with O1 O2 O3 O6 atoms comprising the plane and O7 N1 in vertex position. The Co-O distances are in the range of 2.012(7)-2.200(10) Å[20] and Co-N bond distances is 2.140(8) Å[20c], which are consistent with the reported values. The $odip^{4-}$ ligand is partly deprotonated and features a μ_6:η^1:η^1:η^1:η^1:η^1:η^1 coordination mode. The oxygen O5 from the $odip^{4-}$ ligand lies on a crystallographic twofold axis and the oxygen O7 which is bonded to Co1 lies on another twofold axis. The dihedral angle between the two phenyls is 85.153° with the ether bond angle of 118.34(5) °. The four carboxyl groups in the $odip^{4-}$ ligand connected four $Co_2(CO_2)_4$ units with the Co-Co distance of 2.34 Å. Interestingly, there are two types of 1D channel in the final framework along the *c* axis. The large channel with the poles of 7.3Å×7.3 Å is surrounded by six small channels (Figure 1b and 1c), whereas the small channel is occupied by the coordinated py molecules (Figure 1b). Calculation using PLATON shows that the volume of the MOF **1** is 25.9% of the crystal volume. In terms of the structural topology, the dinuclear $Co_2(CO_2)_4$ unit can be regarded as a 4-coordinated node and the $odip^{4-}$ ligands are linked with four $Co_2(CO_2)_4$ SBUs acting as another 4- coordinated node. The whole structure of the 3D MOF **1** exhibits a 4-coordinated framework with a point symbol for net ($6^5 \cdot 8$) (Figure 1d).

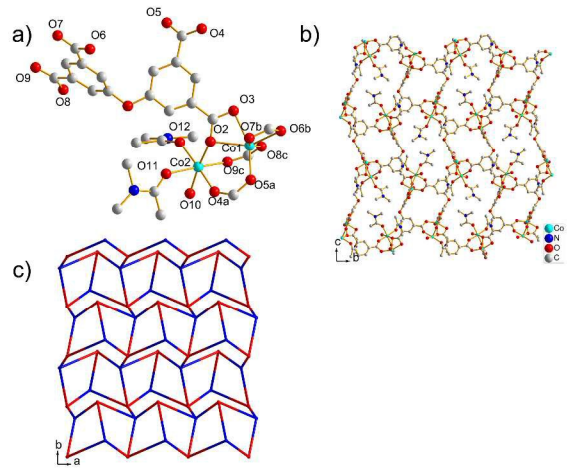

Figure 2 (a) The coordination environment of Co and the bonding mode of the H_4odip in MOF **2**. All H atoms are omitted for clarity. The atoms with superscript 'a' are related by (2-x, -0.5+y,1.5-z), 'b' are related by (2.5-x,2-y,-0.5+z), 'c' are related by (1.5-x,2-y,-0.5+z); (b) The 3D framework of MOF **2**; (c) Schematic representation of the topological net of MOF **2**.

$Co_2(odip)(H_2O)(DMA)_2 \cdot 2DMA$ **(2).** MOF **2** is a 3D framework crystallizing in the orthorhombic space group $P2_12_12_1$. The asymmetric unit contains two independent Co^{2+} atoms, one $odip^{4-}$ ligand, one water molecule and two DMA molecules (Figure 2a). The Co1 atom is six-coordinated by four carboxyl oxygen atoms from four different $odip^{4-}$, forming a distorted octahedral geometry. The Co2 atom is also in octahedral geometry and coordinated with three carboxyl oxygen atoms from three individual ligands, one

oxygen atom from water and two oxygen atoms from DMA. The Co-O bond distances are in the range of 1.970(6) - 2.463(7) Å[20]. Co1 and Co2 are connected by three bridging carboxyl groups with a distance of 3.49 Å, forming the $Co_2(RCO_2)_4$ node. The odip^{4-} ligand in MOF **2** is exhibiting one kind of coordination mode: μ_6:η^1:η^2:η^1:η^1:η^1:η^1. The dihedral angle between two phenyl rings is 72.58(3) ° with the ether bond angle of 117.18(2) °, just the same as ether bond angle in MOF **1**. To better understand the nature of the whole 3D structure of MOF **2**, the topological analysis approach is employed to reduce the multidimensional structure to simple node-and-linker nets[17]. The $Co_2(RCO_2)_4$ SBU in MOF **2** can be simplified as a 4-coordinated node. Each odip^{4-} ligand can be viewed as a 4-coordinated linker. Therefore, from a topological point of view, the final framework of MOF **2** can be regarded as a 4-coordinated net with a point symbol of ($4^2 \cdot 6^3 \cdot 8$), as shown in Figure 2c for MOF **2**.

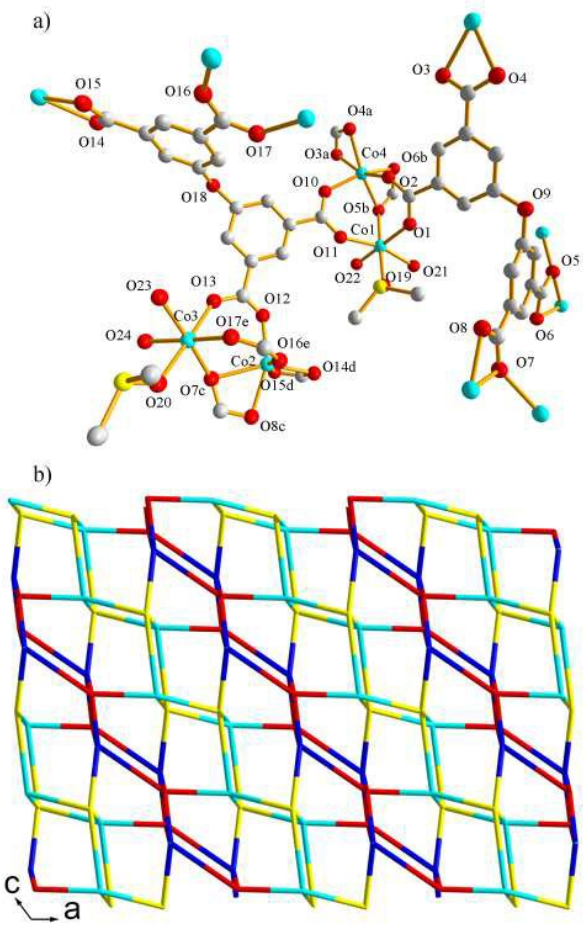

Figure **3** (a) The coordination environment of Co and the bonding mode of the odip^{4-} in MOF **3**. All H atoms are omitted for clarity. The atoms with superscript 'a' are related by (1-x,-0.5+y,1.5-z), 'b' are related by (1-x,1-y,2-z), 'c' are related by (-x,0.5+y,1.5-z) 'd' are related by (x, 0.5-y,0.5+z) and 'e' are related by (-x,1-y,1-z); (b) Schematic representation of the 3D framework topological net of MOF **3**.

$Co_4(odip)_2(H_2O)_4(DMSO)_2 \cdot 5DMSO$ **(3).** The single-crystal X-ray diffraction analysis reveals that MOF **3** crystallizes in the monoclinic space group $P2_1/c$. The asymmetric unit of MOF **3** consists of four crystallographically independent Co^{2+} ions, two coordination odip^{4-} ligands, four coordination water molecules and two coordination DMSO molecules. Co1 is connected with five oxygen atoms from one chelating carboxyl group and three different bridging carboxyl groups. Co4 displays octahedral geometry with six oxygen atoms, three bridging carboxyl groups from different odip^{4-} ligands, two oxygen atoms from coordination water molecules and one oxygen atom from coordination DMSO molecule. Co1 and Co4 are linked by three bridging carboxyl groups and one chelating carboxyl group, forming a binuclear $Co_2(CO_2)_4$ cluster with the Co1-Co4 distance of 3.54 Å. Co3 is connected with six oxygen atoms from two chelating carboxyl groups and two bridging carboxyl groups while Co2 has the same coordination geometry as Co4. Just like the Co1-Co4 cluster, Co2 and Co3 are linked by two bridging carboxyl groups and two chelating carboxyl groups, leading to another binuclear $Co_2(CO_2)_4$ cluster with the Co2-Co3 distance of 3.49 Å. The Co-O and Co-N bond distances are in the range of 1.987(6) -2.260(5) Å[20], which are consistent with the reported values. There are two crystallographically independent ligands with different coordination modes. In mode 1, the odip^{4-} ligand is partly deprotonated and links seven Co atoms, exhibiting a coordination mode of μ_7:η^1:η^1:η^1:η^1:η^1:η^1:η^1 (Figure 7c). In this mode, the dihedral angle between the two phenyls is 85.05(4) ° with the ether bond angle of 115.97(5) °. In mode 2, the odip^{4-} ligand is completely deprotonated and connects with seven Co atoms. The coordination mode of the odip^{4-} ligand is μ_7:η^1:η^2:η^1:η^2:η^1:η^1:η^1:η^1 (Figure 7d). In this mode, the dihedral angle between the two phenyls is 89.31(7) ° with the ether bond angle of 118.19(2) °. Topologically, the two kinds of dinuclear Co clusters and the two types of odip^{4-} ligands can be viewed as a 4-coordinated tetrahedral node (Figure 3b). Therefore, MOF **3** can be rationalized as a 4-coordinated framework with the point symbol of ($4 \cdot 6^4 \cdot 8$)-($4 \cdot 6^5$). Its schematic representation is shown in Figure 3b.

$[Zn_2(odip)(DMF)_2(H_2O)] \cdot 2DMF \cdot 2H_2O$ **(4)**. The single-crystal X-ray diffraction analysis reveals that MOF **4** crystallizes in the monoclinic crystal system with space group $P2_1/c$. The asymmetric unit of MOF **4** consists of two Zn^{2+} atoms, one odip^{4-} ligand molecule, one water molecule, two coordination DMF molecules and two free DMF molecules. From Figure 4a, we can see that Zn1 displays octahedral geometry with three carboxyl oxygen atoms from three individual ligands, one oxygen atom from water and two oxygen atoms from DMF. For Zn2, the tetrahedral coordination environment is completed by four carboxyl oxygen atoms from four different

ligands. Zn1 and Zn2 are connected by three bridging carboxyl groups with the a distance of 3.73 Å, forming the $Zn_2(RCO_2)_4$ node. The Zn-O bond distances fall in the range of 1.946(3)-2.125(3) Å[19]. H_4odip is deprotonated, and features a μ_7:η^1:η^1:η^1:η^1:η^1:η^1:η^1 coordination mode. The four carboxyl groups show two coordination types: bridging μ_2-η^1:η^1 and monodentate μ_1-η^1:η^0 (Figure 4a). There is a 1D channel along the *a* axis which is occupied by DMF molecules. The total potential solvent area is 417.5 $Å^3$, just about 11.2% of the per unit cell

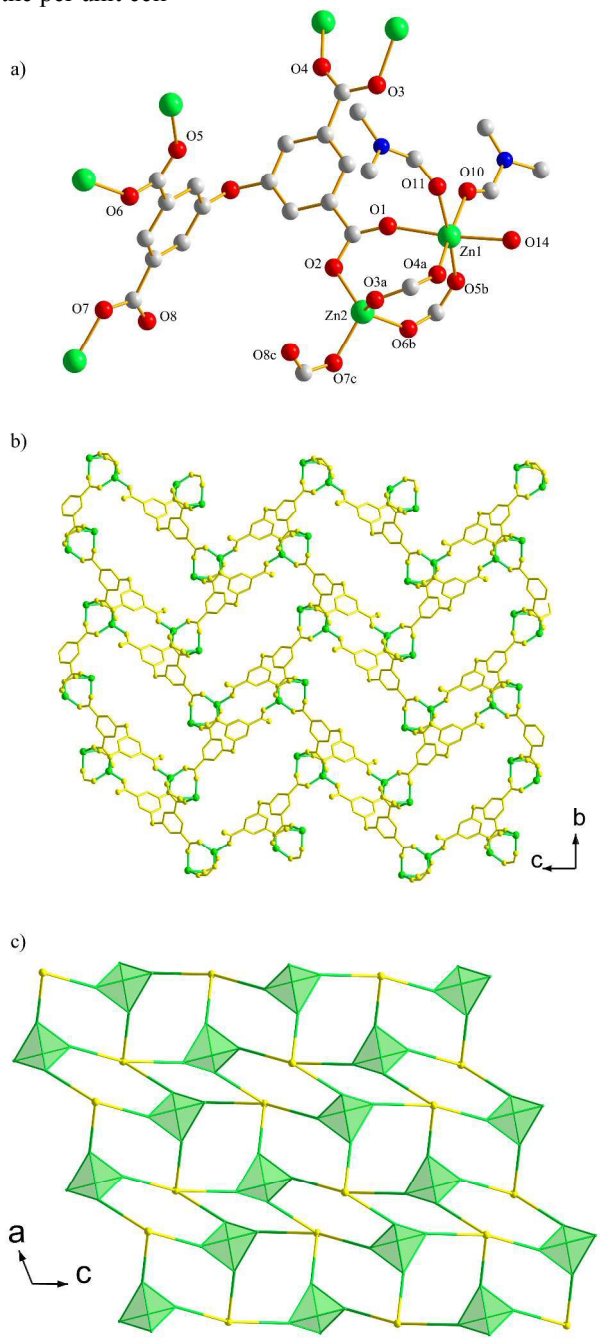

Figure 4 (a) The coordination environment of Zn and the bonding mode of the odip^{4-} in MOF **4**. All H atoms are omitted for clarity. The atoms with superscript 'a' are related by (1-x,0.5+y,-0.5-z), 'b' are related by (1+x,y,-z), 'c' are related by (1-x,-y,-z); (b) The 3D framework of MOF **4**; (d) Schematic representation of topological net of **4**.

volume from the PLATON calculation. The dihedral angle between two phenyl rings is 84.21(3) ° with the ether bond angle of 114.15(5) °, have a slightly rotate compared with MOF **1**. The $Zn_2(RCO_2)_4$ SBU in MOF **4** can be simplified as 4-coordinated node. Each odip^{4-} ligand can be viewed as a 4-coordinated linker. Therefore, from a topological point of view, the final framework of MOF **4** can be regarded as a 4-coordinated net, as shown in Figure 4c, with a point symbol of $(4^2\cdot6^3\cdot8)$, which is the same as that of MOF **2**.

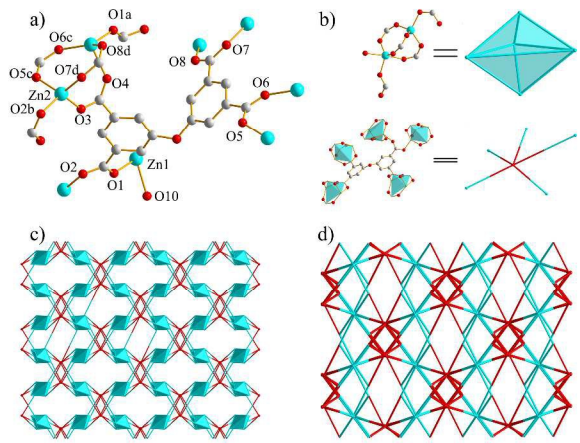

Figure 5 (a) The coordination environment of Zn and the bonding mode of the odip^{4-} in MOF **5**. All H atoms are omitted for clarity, The atoms with superscript 'a' are related by (-0.5-x,2.5-y.-1-z), 'b' are related by (x,2-y,0.5+z), 'c' are related by (-0.5+x,-0.5+y,z) and 'd' are related by (x, 3-y,0.5+z); (b) Defined 5-connected nodes of $[Zn_2(RCO_2)_5]$ SBU and H_4odip ligand; (c) The 3D framework of MOF **5**; (d) Schematic representation of the topological net of MOF **5**.

Zn_2(odip)(H_2O) (5) Single-crystal X-ray diffraction analysis reveals that MOF **5** crystallizes in the monoclinic crystal system with space group *C*2/*c*. The asymmetric unit of MOF **5** contains two crystallographically independent Zn^{2+} atoms, one odip^{4-} ligand and one water molecule. As shown in Figure 5a, the Zn1 atom is 5-coordinated and surrounded by four carboxyl oxygen atoms from four individual odip^{4-} ligands and one atom from coordinated water molecule, forming a twin-triangle-prick geometry. The triangle plane is formed by the coordination of O1, O2 and O6 atoms. The axial positions are occupied by O10 and O4 atoms with a O4−Zn1−O10 bond angle of 171.58(11) °. The Zn1−O bond distances are 1.942(2)-2,166(3) Å[19]. The Zn2 atom adopts a tetrahedral geometry, coordinated by four carboxyl oxygen atoms from four different odip^{4-} ligands. The Zn2-O bond distances are 1.935(3)-1.970(2) Å[19]. Zn1 and Zn2 are connected by three bridging carboxyl groups with a distance of 3.44 Å. At the

same time, each Zn atom is connected with a μ_2-η^1:η^1 carboxylic group forming the $Zn_2(RCO_2)_5$ node (Figure 5b). It is worth noting that the $[Zn_2(RCO_2)_5]$ SBU is surrounded by five odip^{4-} ligands, which can be viewed as a 5-coordinated net. The odip^{4-} ligand is octadentate and coordinates to eight Zn^{2+} ions via four chelating carboxyl groups through the μ_8:η^1:η^1:η^1:η^1:η^1:η^1:η^1:η^1 coordination mode (Figure 5b). The dihedral angle between two phenyl rings is 74.35 (4) ° with the ether bond angle of 118.95(1) °. Each odip^{4-} ligand links five different $[Zn_2(RCO_2)_5]$ SBUs (Figure 5b). From the viewpoint of topology, the whole 3D framework exhibits a 5-coordinated net. The extended point symbol for this network is $(4^4 \cdot 6^6)$ (Figures 5c and 5d).

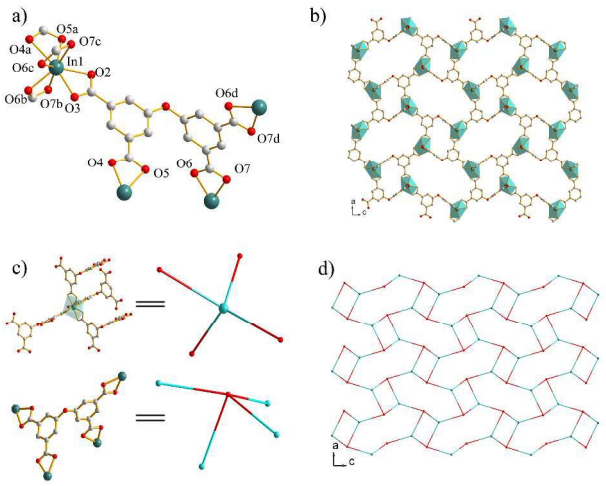

Figure 6 (a) The coordination environment of In and the bonding mode of the odip^{4-} in MOF **6**. All H atoms are omitted for clarity. The atoms with superscript 'a' are related by (-0.5+x,-0.5-y.1.5-z), 'b' are related by (0.5-x,-y,0.5+z), 'c' are related by (0.5-x,-0.5+y,0.5+z) and 'd' are related by (x, -0.5-y, z); (b) The 3D framework of MOF **6**; (c) Defined 4-connected nodes of $In(RCO_2)_4$ and H_4odip ligand; (d) Schematic representation of the topological net of MOF **6**.

In(odip)·3ACN **(6)**. Complex **6** crystallizes in the orthorhombic crystal system with space group *Pnma* and exhibits a 3D framework. The asymmetric unit of MOF **6** consists of half of an indium atom and half of a ligand molecule. As shown in Figure 6a, the indium ion is surrounded by eight oxygen atoms from four different μ_1-η^1:η^1-chelate carboxylate groups of four odip^{4-} ligands, generating a octahedral geometry $In(RCO_2)_4$ secondary building unit. The In–O bond distance lies in the range of 2.182(6)–2.419(7)Å, which is in good agreement with previous studies[17]. The deprotonated H_4odip ligand adopts a μ_4:η^1:η^1:η^1:η^1:η^1:η^1:η^1:η^1 coordination mode (Figure 6a) and links four In^{3+} atoms as shown in Figures 6a and 6b. The dihedral angle between two phenyl rings is 90.01(4) ° with an ether bond angle of 117.20(1) °. At the same time, there are two kinds of channels along the *b* axis. The dimensions of the smaller and bigger channels are about 4.1 Å × 6.4 Å and 7.4 Å × 9.3 Å, respectively, with the dimethylamine cation molecules omitted, and the PLATON analysis shows that the 3D porous structure has a solvent area volume of 2642.1 Å^3, about 68.7% per unit cell volume. The $In(RCO_2)_4$ SBU in MOF **6** (Figure 6c) can be simplified as a 4-coordinated node. Each odip^{4-} ligand can be viewed as a 4-coordinated linker. Therefore, from a topological point of view, the final framework of MOF **6** can be regarded as a 4-coordinated net with a point symbol of $(4^2 \cdot 6^3 \cdot 8)$, as shown in Figure 6d, just the same as that of MOFs **2** and **4**.

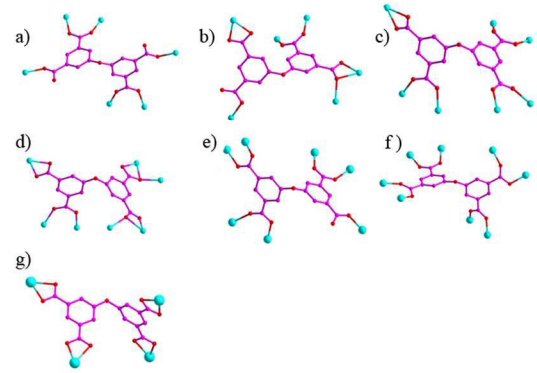

Figure 7 Coordination modes of H_4odip in MOFs **1**–**6**.

Coordination modes of the H_4odip ligand in MOFs 1–6

The coordination geometry of H_4odip ligands is found to be greatly influenced by the central metals and the solvent environment in the formation of the final structures. Based on the structural descriptions of MOFs **1-6**, the two phenyl rings in one H_4odip ligand rotate through the flexible ether band. There are seven coordination modes in these six MOFs (Figure 7).The H_4odip ligands in MOF **1** (Figure 7a), MOF **2** (Figure 7b) and MOF **4** (Figure 7e) are partly deprotonated while in MOF **3** (Figures 7c and 7d), MOF **5**(Figure 7f) and MOF **6**(Figure 7g) are fully deprotonated. In MOFs **1** and **2**, all the H_4odip ligands coordinate with six Co^{2+} ions in different fashions, for μ_6:η^1:η^1:η^1:η^1:η^1:η^1 mode in MOF **1** and μ_6:η^1:η^2:η^1:η^1:η^1:η^1:η^1 in MOF **2**. In MOF **3**, the H_4odip ligand links seven Co^{2+} ions in two coordinate modes: μ_7:η^1:η^1:η^1:η^1:η^1:η^1:η^1:η^1 and μ_7:η^1:η^2:η^1:η^2:η^1:η^1:η^1:η^1, resulting in a 3D framework. In MOF 4, the H_4odip ligand links seven Zn^{2+} ions in a fashion of μ_7:η^1:η^1:η^1:η^1:η^1:η^1:η^1 coordination mode, which is slightly different from MOF **3**. For MOF **5**, the H_4odip ligand features a μ_8:η^1:η^1:η^1:η^1:η^1:η^1:η^1:η^1 coordination mode and links eight Zn^{2+} ions. In MOF **6**, four In3+ ions are linked by one H_4odip ligand with the μ_4:η^1:η^1:η^1:η^1:η^1:η^1:η^1:η^1 coordination mode. The structure of MOFs **1-3**, suggests that they have the same coordination numbers of Co^{2+} and the coordination solvent plays an important role in causing the distinction in the final structural topology. For MOF **1** and MOF **3**, they have the same DMSO solvent with pyridine in MOF **1** but water in MOF **3**. For MOF **2,** DMA replaced the DMSO in MOF **3** with the same water. The change in the coordination solvent affects the coordination environment of the central metals and

the ligands, leading to different final structures. For MOFs **4** and **5**, different zinc salts were added. The difference in the final structures of them may be caused by the change of anions.

Luminescent properties.

Luminescent MOFs have attracted intense interest for their potential applications in photochemistry, chemical sensors and electroluminescent. In this study, the solid-state luminescent properties, including excited/emissive spectra, of free H_4odip ligand and MOF **4** as well as MOF **5** were investigated at room temperature under the same experimental conditions. As shown in Figure 8, the strong emission peak for the H_4odip is observed at 445 nm upon excitation at 290 nm. When excited at 290 nm, the emission maximum of MOF **4** and MOF **5** is found to be at 483 nm and 490 nm, respectively, with a small red shift relative to the H_4odip ligand, which could be attributed to the π−π* charge transition within the aromatic rings of the ligand[21]. Meanwhile, the fluorescent intensity of MOF **4** and MOF **5** has distinctly increased compared with the H_4odip ligand, which may be due to the coordination of metal clusters to the ligand, resulting in increased rigidity of the ligand and reduced non-radioactive loss[22].

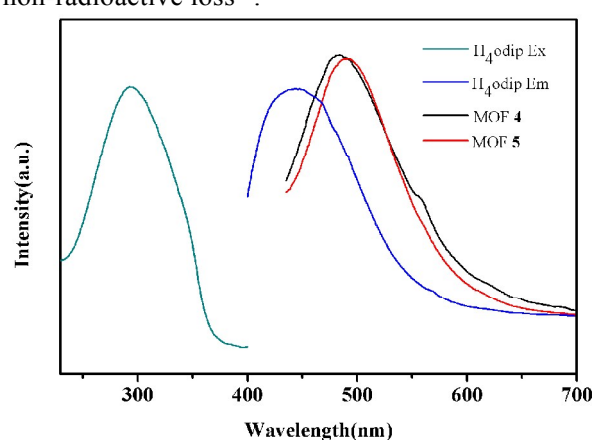

Figure 8 Photoluminescence of H_4odip ligand, MOF **4** and MOF **5**.

Magnetic properties

The magnetic susceptibilities, χM, of MOFs **1**−**3** have been measured in the 2−300 K temperature range with magnetic field of 1000Oe and the magnetic properties of MOFs **1**-**3** in the form of $\chi_M T$, χ_M, and $1/\chi_M$ are shown in Figure 9 respectively. At room temperature, the $\chi_M T$ of MOF **1** is 5.62 $cm^3 K\ mol^{-1}$, which is significantly larger than the spin-only value for two isolated Co^{2+} ions (3.75 $cm^3 K mol^{-1}$ and $S=^3/_2$) and the $\chi_M T$ value keeps almost constant until about 50 K, then decreases sharply to 0.99 $cm^3 K\ mol^{-1}$ at 2K upon further cooling. The decrease of $\chi_M T$ in the low temperature range indicates the weak antiferromagnetic interaction between the Co^{2+} ions. The temperature dependence of the reciprocal susceptibilities ($1/\chi_M$) of MOF **1** obeys the Curie−Weiss law with $\chi_M = C/(T - \theta)$, with $\theta = -1.21$ K, C = 5.17 $cm^3\ K\ mol^{-1}$. The negative θ value also indicates the presence of weak antiferromagnetic interactions among adjacent Co^{2+} ions and /or the spin−orbit coupling effect coming from Co^{2+} ions in MOF **1**[23]. Two adjacent dinuclear Co_2 units are separated by $odip^{4-}$ ligands. Therefore, the magnetic interactions can be considered to exist only between two adjacent metal ionsbridged by carboxylate groups and the interactions between two adjacent dinuclear Co_2 units can be ignored.

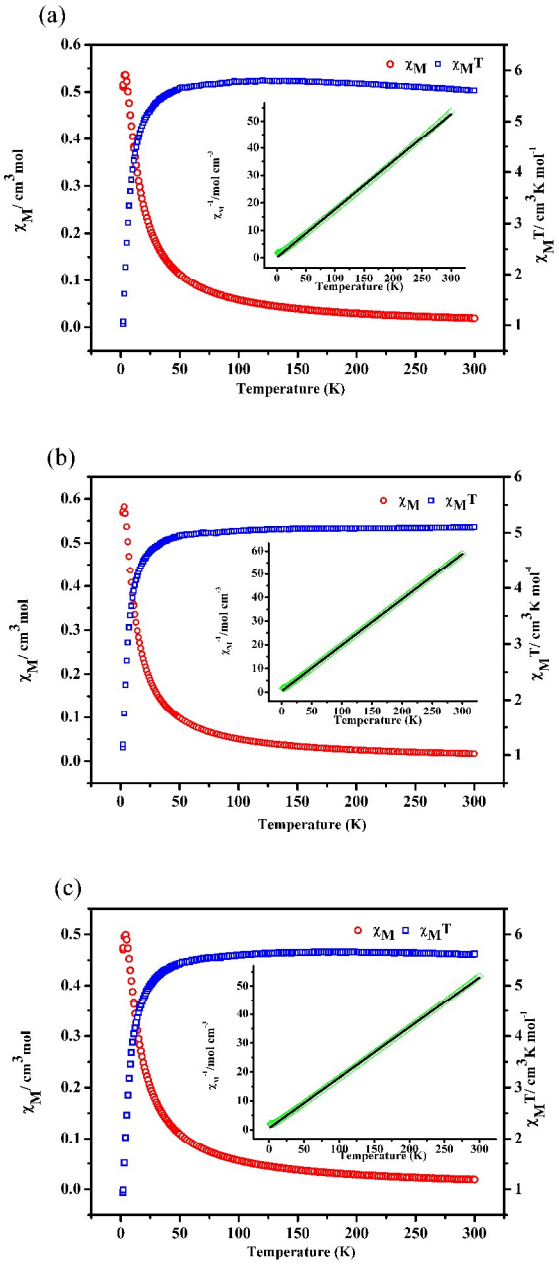

Figure 9 (a) The $\chi_M T$, χ_M, and $1/\chi_M$ vs T plots for MOF **1**, (b) The $\chi_M T$, χ_M, and $1/\chi_M$ vs T plots for MOF **2** and (c) The $\chi_M T$, χ_M, and $1/\chi_M$ vs T plots for MOF **3**. The red line represents the best fits.

For MOFs **2** and **3**, the $\chi_M T$ is equal to 5.10 and 5.61 cm^3 K

mol^{-1} respectively at room temperature. Just like MOF **1**, the χ_MT is much higher than the spin-only value for two isolated Co^{2+} ions but lies in the observed range for Co^{2+} complexes. The χ_MT solwly decreases to 4.94 and 5.44 cm^3 K mol^{-1} respectively at 50K. Upon cooling, χ_MT decreases rapidly to 1.13 and 0.94 cm^{3}K mol^{-1} at 2 K. The decrease of χ_MT could be attributed to the antiferromagnetic coupling between the Co^{2+} ions. The temperature dependence of the reciprocal susceptibilities ($1/\chi_M$) of MOFs **2** and **3** also fits the Curie−Weiss law with $\theta = -2.89$ K, C = 5.15 cm^3 K mol^{-1} for MOF **2** and $\theta = -3.25$K, C = 5.72 cm^3 K mol^{-1} for MOF **3**. The negative θ value suggests antiferromagnetic interactions among adjacent Co^{2+} ions and /or the spin−orbit coupling effect coming from Co^{2+} ions in MOF **2** and **3.**

Conclusions

In summary, based on the flexible tetracarboxylate ligand H_4odip, six novel metal-organic frameworks named $Co_2O(odip)(py)_2(DMSO)_2$ (**1**), $Co_2(odip)(H_2O)(DMA)_2$ (**2**), $Co_4(odip)_2(H_2O)_4(DMSO)_2$ (**3**), $[Zn_2(odip)(DMF)_2(H_2O)]\cdot 2DMF$(**4**), $Zn_2(odip)(H_2O)$ (**5**) and In(odip) (**6**) have been synthesized with different metal salts in solvothermal conditions and characterized by single-crystal X-ray diffraction. MOF **1** possesses a 3D 4-coordinated architecture with $(6^5\cdot 8)$ topology. MOFs **2**, **4** and **6** feature 3D 4-coordinated nets with $(4^2\cdot 6^3\cdot 8)$ topology. MOF **3** shows a 3D interpenetrated 4-coordinated framework with $(4\cdot 6^4\cdot 8)(4\cdot 6^5)$ topology. MOF **5** exhibits a 3D 5-coordinated framework with $(4^4\cdot 6^6)$ topology. It is found that the solvent affects the coordination environment of central metals and the ligands, and plays important roles in the formation of the final structural topology framework of MOFs **1**, **2** and **3**. For MOFs **4** and **5**, different zinc salts were added. The final structures were affected by the change of anions. Moreover, MOFs **4** and **5** can serve as good candidates for photoactive materials, owing to their strong luminescent emissions. The temperature-dependent magnetic measurements reveal weak antiferromagnetic interactions between Co^{2+} centers in MOFs **1**, **2** and **3**. Further work using Ln CPs and flexible tetracarboxylate ligands is in progress in our lab.

Acknowledgements

This work was supported by the National Natural Science Foundation of China (no.21371069), the Graduate Innovation Fund of Jilin University (no.2014008), the Specialized Research Fund for the Doctoral Program of Higher Education (no.20110061110015) and the National High Technology Research and Development Program of China (863 program) (no.2013AA031702).

Notes and references

State Key Laboratory of Inorganic Synthesis and Preparative Chemistry,
College of Chemistry, Jilin University, Changchun, 130012, PR China.
E-mail: zshi@mail.jlu.edu.cn; Fax: +86 431 85168624; Tel: +86 431 85168662;

† Electronic Supplementary Information (ESI) available: CCDC reference numbers 1032697–1032699 for MOFs **1-3**,1032695 for **4**, 1032696 for **5**, and 1032694 for **6**. The PXRD patterns, the FTIR and the TGA plot of MOFs **1-6** .For ESI and crystallographic data in CIF or other electronic format see DOI: 10.1039/b000000x/

1 (a) X. Z. Li, M. Li, Z. Li, J. Z. Hou, X. C. Huang and D. Li, *Angew. Chem., Int. Ed.*, 2008, **47**, 6371; (b) O. M. Yaghi, M. O'Keeffe, N. W. Ockwig, H. K. Chae, M. Eddaoudi and J. Kim, *Nature*., 2003, **423**, 705; (c) Z. Y. Guo, H. Xu, S. Q. Su, J. F. Cai, S. Dang, S. C. Xiang, G. D. Qian, H. J. Zhang, M. O'Keefe and B. L. Chen, *Chem. Commun*., 2011, **47**, 5551; (d) Y. S. Wei, R. B. Lin, P. Wang, P. Q. Liao, C. T. He, W. Xue, L. Hou, W. X. Zhang, J. P. Zhang and X.-M. Chen, *CrystEngComm*, 2014, **16**, 6325; (e) M. Li, D. Li, M. O'Keeffe and O. M. Yaghi, *Chem. Rev.,* 2014, **114**, 1343.

2 (a) L. Du, Z. Lu, K. Zheng, J. Wang, X. Zheng, Y. Pan, X. You and J. Bai, *J. Am. Chem. Soc.*, 2012, **135**, 562; (b) M. Wriedt, J. P. Sculley, A. A. Yakovenko, Y. Ma, G. J. Halder, P. B. Balbuena and H. C. Zhou, *Angew. Chem., Int. Ed.*, 2012, **51**, 9804; (c) J. R. Li, J. Sculley and H. C. Zhou, *Chem. Rev*., 2012, **112**, 869; (d) B. Wang, A. P. Cote, H. Furukawa, M. O'Keeffe and O. M. Yaghi, *Nature*, 2008, **453**, 207; (d) K. Sumida, D. L. Rogow, J. A. Mason, T. M. McDonald, E. D. Bloch, Z. R. Herm, T. H. Bae and J. R. Long, 35 *Chem. Rev*., 2012, **112**, 724.

3 (a) Q. Yang, X. Chen, J. Cui, J. Hu, M. Zhang, L. Qin, G. Wang, Q. Lu and H. Zheng, *Cryst. Growth Des.*, 2012, **12**, 4072; (b) X. N. Cheng, W. X. Zhang, Y. Y. Lin, Y. Z. Zheng and X. M. Chen, *Adv. Mater*., 2007, **19**, 1494; (c) S. C. Xiang, X. T. Wu, J. J. Zhang, R. B. Fu, S. M. Hu and X. D. Zhang, *J. Am. Chem. Soc.*, 2005, **127**, 16352.

4 (a) C. Wang, Z. Xie, K. E. deKrafft and W. Lin, *J. Am. Chem. Soc.*, 2011, **133**, 13445; (b) M. Yoshizawa, M. Tamura and M. Fujita, *Science*, 2006, **312**, 251; (c) M. D. Allendorf, C. A. Bauer, R. K. Bhakta and R. J. T. Houk, *Chem. Soc. Rev*., 2009, **38**, 1330; (d) L. Ma, C. Abney and W. Lin, *Chem. Soc. Rev*., 2009, **38**, 1248.

5 (a) L. E. Kreno, K. Leong, O. K. Farha, M. Allendorf, R. P. Van Duyne and J. T. Hupp, *Chem. Rev*., 2012, **112**, 1105; (b) C. A. Bauer, T. V. Timofeeve, T. B. Settersten, B. D. Parrerson, V. H. Liu, B. A. Simmons and M. D. Allendorf, *J. Am. Chem. Soc.*, 2007, **129**, 7136;(c) Su, S.; Chen, W.; Qin, C.; Song, S.; Guo, Z.; Li, G.; Song, X.; Zhu, M.; Wang, S.; Hao, Z. and Zhang, H. *Cryst. Growth Des*., 2012, **12**, 1808.

6 (a) P. Horcajada, C. Serre, M. Vallet-Regi, M. Seban, F. Taulelle and G. Fe´rey, *Angew. Chem., Int. Ed.*, 2006, **45**, 5974; (b)S. R. Miller, D. Heurtaux, T. Baati, P. Horcajada, J.-M. Greneche and C. Serre, *Chem. Commun*., 2010, **46**, 4526.

7 (a) W. Liu, L. Ye, X. Liu, L. Yuan, J. Jiang and C. Yan, *CrystEngComm*, 2008, 10, 1395; (b) L. Y. Park, D. G. Hamilton, E. A. McGehee and K. A. McMenimen, *J. Am. Chem. Soc.*, 2003, **125**, 10586; (c) B. Chen, S. Ma, F. Zapata, E. B. Lobkovsky and J. Yang, *Inorg. Chem*., 2006, **45**, 5718; (d) H. L. Gao, L. Yi, B. Zhao, X. Q. Zhao, P. Cheng, D. Z. Liao and S. P. Yan, *Inorg. Chem.*, 2006, **45**,

5980; (e) A. D. Burrows, R. W. Harrington, M. F. Mahon and S. J. Teat, *Cryst. Growth Des.*, 2004, **4**, 813.

8 (a) Zhao, F. H.; Jing, S.; Che, Y. X.; Zheng, J. M. *CrystEngComm.,* 2012, **14**, 4478; (b) Y. W. Li, H. Ma, Y. Q. Chen, K. H. He, Z. X. Li and X. H. Bu, *Cryst Growth Des.*, 2012, **12**, 189; (c) L. Fan, X. Zhang, W. Zhang, Y. Ding, W. Fan, L. Sun and X. Zhao, *CrystEngComm.*, 2014, **16**, 2144;(d) L. Fan, X. Zhang, W. Zhang, Y. Ding, W. Fan, L. Sun, Y. Pang and X. Zhao, *Dalton Trans.*, 2014, **43**, 6701;(e) L. Shen, D. Gray, R. I. Masel and G. S. Girolami, *CrystEngComm*, 2012, **14**, 5145;(f) X. He, X. P. Lu, Z. F. Ju, C. J. Zhang, Q. K. Zhang and M. X. Li, *CrystEngComm.*, 2013, **15**, 2731

9 (a)D. Yuan, D. Zhao, D. Sun and H. C. Zhou, *Angew. Chem., Int. Ed.*, 2010, **49**, 535 ; (b) J. T. Jia, F. X. Sun, T. Borjigin, H. Ren, T. T. Zhang, Z. Bian, L. Gao and G. S. Zhu, *Chem. Commun.*, 2012, **48**, 6010;(c) S. Kitagawa, R. Kitaura and S. Noro, *Angew. Chem. Int. Ed.,* 2004, **43**, 2334.

10 (a) J. Luo, J. Wang, G. Li, Q. Huo and Y. Liu, *Chem. Commun.*, 2013, **49**, 11433; (b) H. Furukawa, N. Ko, Y. B. Go, N. Aratani, S. B. Choi, E. Choi, A.O. Yazaydin, R. Q. Snurr, M. O'Keeffe, J. Kim and O. M. Yaghi, *Science.*, 2010, **329**, 424.

11 (a)J. H. Cui, Y. Z. Li, Z. J. Guo and H. G. Zheng, *Chem. Commun.*, 2013, **49**, 555; (b) N. Wei, M. Y. Zhang, X. N. Zhang, G. M. Li, X. D. Zhang and Z. B. Han, *Cryst. Growth Des.*, 2014, **14**, 3002; (c) X. Zhang, L. Hou, B. Liu, L.Cui, Y.Y. Wang and B. W, *Cryst. Growth Des.*, 2013, **13**, 3177.

12 (a) Y. Y. Liu, Z. H. Wang, J. Yang, Y. Y. Liu and J. F. Ma, *CrystEngComm.*, 2011, **13**, 3811; (b) R. Singh, J. Mrozinski, and P. K. Bharadwaj, *Crystal Growth & Design.*, 2014, **14**, 3623

13 (a)B. Y. Li, Z. J. Zhang, Y. Li,K.X.Yao, Y. H. Zhu, Z. Y. Deng, F. Yang, X. J. Zhou, G. H. Li, H. H. Wu, N. Nijem, Y. J. Chabal, Z. P. Lai, Y. Han, Z. Shi, S. H. Feng and J. Li, *Angew. Chem., Int. Ed.*, 2012, **51**, 1212; (b)K. Liu, B. Y. Li, Y. Li, X. Li, F. Yang, G. Zeng, Y. Peng, Z. J. Zhang, G. H. Li, Z. Shi, S. H. Feng and D. T. Song, *Chem. Commun.*, 2014, **50**, 5031; (c) K. Liu, Y. Peng, F. Yang, D. X. Ma, G. H. Li, Z. Shi and S. H. Feng, *CrystEngComm.*, 2014, **16**, 4382.

14 P. Lama, A. Aijaz, E. C. sanudo and K.Bharadwaj, *Crystal Growth & Design.*, 2010, **10**, 283.

15 G. M. Sheldrick, *SHELXTL-97*, Program for Crystal Structure Refinement, University of Göttingen, 1997.

16 A. L. Spek, *Acta Cryst.*.,2015, C**71**, 9-18.

17 V. A. Blatov, Multipurpose crystallochemical analysis with the program package TOPOS*, IUCr Comp. Comm. Newsl.*, 2006**,7**, 4.

18 (a) S. Wang, T. Zhao, G. Li, L. Wojtas, Q. Huo, M. Eddaoudi and Y. Liu, *J. Am. Chem. Soc.*, 2010, **132**, 18038; (b) S. T. Zheng, J. T. Bu, Y. Li, T. Wu, F. Zuo, P. Feng and X. Bu, *J. Am. Chem. Soc.*, 2010, **132**, 17062.

19 (a)S. L. Li, K. Tan, Y. Q. Lan, J. S. Qin, M. N.Li, D.Y. Du and Z. M.Su, *CrystEngComm.*, 2011, **13**, 4945;(b) K. L. Mulfort, O. K. Farha, C. L. Stern, A. A. Sarjeant, and J.T. Hupp, *J. Am. Chem. Soc.*, 2009, **131**, 3866;(c) R.R. Zeng, Q. G. Zhai, S.N. Li, Y.C. Jiang and M.C. Hu, *CrystEngComm.*, 2011, **13**, 4823.

20 (a) M. H. Zeng, Y. X. Tan,Y. P. He, Z. Yin, Q. Chen and M. Kurmoo, *Inorg. Chem.*, 2013, **52**, 2353; (b) C. Heering, I. Boldog, V. Vasylyeva, J. Sanchiz and C. Janiak, *CrystEngComm.*, 2013, **15**,9757; (c) S. Sanda, S. Parshamoni, A. Adhikary and Sanjit Konar *Cryst. Growth Des.*, 2013, **13**, 5442; (d) S.Y. Ke, Y. F. Chang, H.Y. Wang, C. C. Yang, C. W. Ni, G. Y. Lin, T. T. Chen, M. L. Ho, G. H. Lee, Y. C. Chuang and C.C. Wang, *Cryst. Growth Des.*, 2014, **14**, 4011.

21 (a) Y. J. Mu, G. Han, S. Y. Ji, H. W. Hou and Y. T. Fan, *CrystEngComm.*, 2011, **13**, 5943; (b) J. Yu, Y. Cui, C. Wu, Y. Yang, Z. Wang, M. O'Keeffe, B. Chen and G. Qian, *Angew. Chem., Int. Ed.*, 2012, **51**, 10542;(c) X.-J. Li, F. L. Jiang, M. Y. Wu, S. Q. Zhang, Y. F. Zhou and M. C. Hong, *Inorg. Chem.*, 2012, **51**, 4116.

22 (a) H. Y. Liu, B. Liu, J. Yang, Y. Y. Liu, J. F. Ma and H. Wu, *Dalton Trans.*, 2011, **40**, 9782; (b) D. Tian, Y. Li, R. Y. Chen, Z. Chang, G. Y. Wang and X. H. Bu, *J. Mater. Chem. A*, 2014, **2**, 1465; (c) S. L. Zheng, J. H. Yang, X. L. Yu, X. M. Chen and W.T. Wong, *Inorg. Chem.*, 2003, **43**, 830.

23 (a) Z. Chen, B. Zhao, P. Cheng, X. Q. Zhao, W. Shi and Y. Song, *Inorg. Chem.*, 2009, **48**, 3493;(b) Xu, Y. Q.; Yuan, D. Q.; Wu, B. L.; Han, L.; Wu, M. Y.; Jiang, F. L.; Hong, M. C. *Cryst. Growth Des.*, 2006, **6**, 1168.